

# Half-kilowatt high energy third harmonic conversion to 50 J @ 10 Hz at 343 nm

Jan Pilar <sup>1</sup>, Martin Divoky <sup>1</sup>, Jonathan Phillips <sup>2</sup>, Martin Hanus <sup>1</sup>, Petr Navratil <sup>1</sup>, Ondrej Denk <sup>1</sup>, Patricie Severova <sup>1</sup>, Tomas Paliesek <sup>1</sup>, Danielle Clarke <sup>2</sup>, Martin Smrz <sup>1</sup>, Thomas Butcher <sup>2</sup>, Chris Edwards <sup>2</sup> and Tomas Mocek <sup>1</sup>

<sup>1</sup> *HiLASE Centre, Institute of Physics of the Czech Academy of Sciences, Za Radnici 828, 25241, Dolni Brezany, Czech Republic*

<sup>2</sup> *Central Laser Facility, STFC Rutherford Appleton Laboratory, Didcot, OX11 0QX, UK*

**Abstract** We report on frequency tripling of high energy, high repetition rate ns pulses from a cryogenically gas cooled multi-slab Yb:YAG laser system Bivoj/DiPOLE, using a type-I phase matched LBO crystal for second harmonic generation and type-II phase matched LBO crystal for sum frequency generation. We achieved conversion to 343 nm with stable energy of 50 J at repetition rate of 10 Hz and conversion efficiency of 53%.

*Key words: diode pumped solid state laser, frequency conversion, high energy lasers, high average power lasers*

## I. INTRODUCTION

With rapid development of high energy and high average power lasers (HE-HAP) diode pumped laser systems, harmonic frequency conversion is tool to broaden application spectrum of such lasers. Recent advances with indirectly driven thermonuclear fusion bring fusion power plant closer to our reach [1], which will require UV lasers with high repetition rate. Such lasers will need optical components LIDT tested with large aperture beam [2–3]. Other applications include

annealing of Silicone to improve its electrical properties for semiconductor industry [4]. And with ultra short pulses, UV micromachining [5], UV ablation [5] and UV air ionization [5] offer performance increase over IR laser pulses.

Phillips et al. demonstrated 65 W of average power with energy of 65 J at 343 nm using multi slab laser system DiPOLE100 and harmonic conversion in lithium triborate (LBO) [6]. Rothhardt et al. demonstrated 100 W of average power and pulse energy of 28.5 uJ at 343 nm with femtosecond fiber laser and subsequent harmonic conversion in beta barium borate (BBO) crystals [7]. Andral et al. generated 120 W of average power and pulse energy of 118 mJ using thin disk picosecond laser and harmonic conversion in LBO crystals [8].

In this paper we report Third Harmonic Generation (THG) of 55 J at repetition rate of 10 Hz from laser system Bivoj/DiPOLE, which corresponds to 550 W of average power and more than 4 times increase to the state-of-the-art. Conversion efficiency of 60% was achieved by using flat top beam and pulse profiles and by successful optimization of thermally induced polarization changes by polarimetric method [9]. After thermal stabilization, the third harmonic energy dropped to around 50 J at 10 Hz. Further increase of the energy at 343 nm was limited by energy available at the fundamental wavelength.

## **II. EXPERIMENT**

The frequency doubled output from a high average power Yb:YAG laser system Bivoj/DiPOLE at 515 nm was converted to 343 nm using residual light at fundamental wavelength of 1030 nm and type II phase matching in LBO crystal. The setup for conversion to 515 nm was described in the previous paper [10] and used sealed oven for temperature stabilization of LBO crystal, which resulted in better conversion stability. After the first LBO crystal, the second LBO crystal (Coherent Inc.) was inserted to perform sum frequency generation. The crystal had an aperture of

$60 \times 60 \text{ mm}^2$ , thickness of 12 mm and cut angles  $\theta$  of  $50.4^\circ$  and  $\varphi$  of  $90^\circ$ . Dual Band Anti-Reflection (DBAR) coating for 1030 nm and 515 nm was used on the front face to minimize reflection to 0.1% and 0.15%, respectively. Single Layer Anti-Reflection (SLAR) coating for 343 nm was used on the back face to minimize reflection to less than 1.5% at 343 nm. Reflection values of the SLAR coating at 1030 nm and 515 nm were 1% and 2.5%, respectively. The crystal was placed into the windowless oven (IB Photonics) for temperature stabilization. The temperature was set to  $30^\circ\text{C}$  for both ovens, as it provided the highest conversion efficiency.

The laser beam from Bivoj laser system is propagated to harmonic conversion setup through two Keplerian telescopes. To increase the energy fluence on the crystal, the telescope de-magnifies the laser beam size 1.56 times from  $77 \times 77 \text{ mm}^2$  to  $49 \times 49 \text{ mm}^2$ . The layout of the harmonic conversion setup is shown in Figure 1 and was described in our previous paper [11].

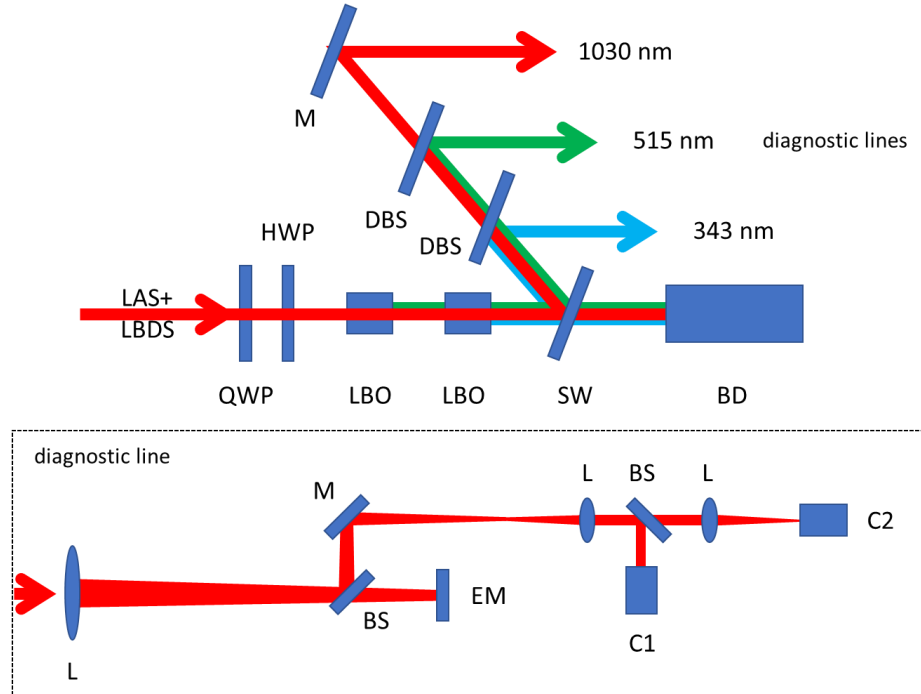


**Figure 1** Schematic layout of the conversion experiment. The laser beam is coming from the laser system via laser beam distribution system (LAS+LBDS). Single components of the setup are denoted as: quarter waveplate (QWP), half waveplate (HWP), conversion crystals (LBO), partially reflecting sampling wedge (SW) and beam dump (BD). Diagnostics consists of dichroic beamsplitter (DBS), mirrors (M), lenses (L), beamsplitters (BS), energy meter

(EM), near field camera (C1) and far field camera (C2 – not present during the experiment). The layout of diagnostic lines is the same for all three wavelengths and is shown only once.

A pair of zero order waveplates ( $\lambda/2$ ,  $\lambda/4$ ) was used to compensate thermally induced polarization changes and adjust polarization at the input of the crystal to improve the conversion efficiency by maximizing the energy in the polarization parallel with the principal plane of the crystal. After passing through the conversion crystals, the beams at 1030 nm, 515 nm and 343 nm wavelengths were absorbed in a beam dump realized by colored glass filters suspended in a water tank. In front of the beam dump a sampling wedge (dielectrically coated  $R \sim 1\%$  at 1030 nm, 515 nm and 343 nm) was placed so that a low power reflection could be acquired and used for diagnostics. The single components of the diagnostic beam were separated according to their wavelengths by a pair of dichroic mirrors. Each diagnostic line consisted of an energy meter (Gentec-EO QE25LP) and a diagnostic camera (AVT Manta 145B) to monitor image-relayed beam profile.

The energy meters were calibrated so that they would show the energy values present at the sampler for any of the three wavelengths. The calibration coefficients for the input (1030 nm), the unconverted fundamental (1030 nm) and second harmonic (515 nm) energy meters remained constant during the whole experiment. However, the calibration coefficient for the third harmonic frequency (343 nm) varied by more than 20% throughout the experiment. Evolution of calibration coefficients is shown in Figure 2. We suspect the cause was the change of reflectivity of the sampling wedge due to heating by the UV laser light. Because of the  $3\omega$  energy meter coefficient uncertainty, we decided to estimate the third harmonic energy as the difference between the input energy and the sum of energies of unconverted fundamental and second harmonic frequencies. All energy readings were corrected to the transmission of the LBO crystals and their coatings at the given wavelengths. We plan to investigate this phenomenon further in a follow-up work.

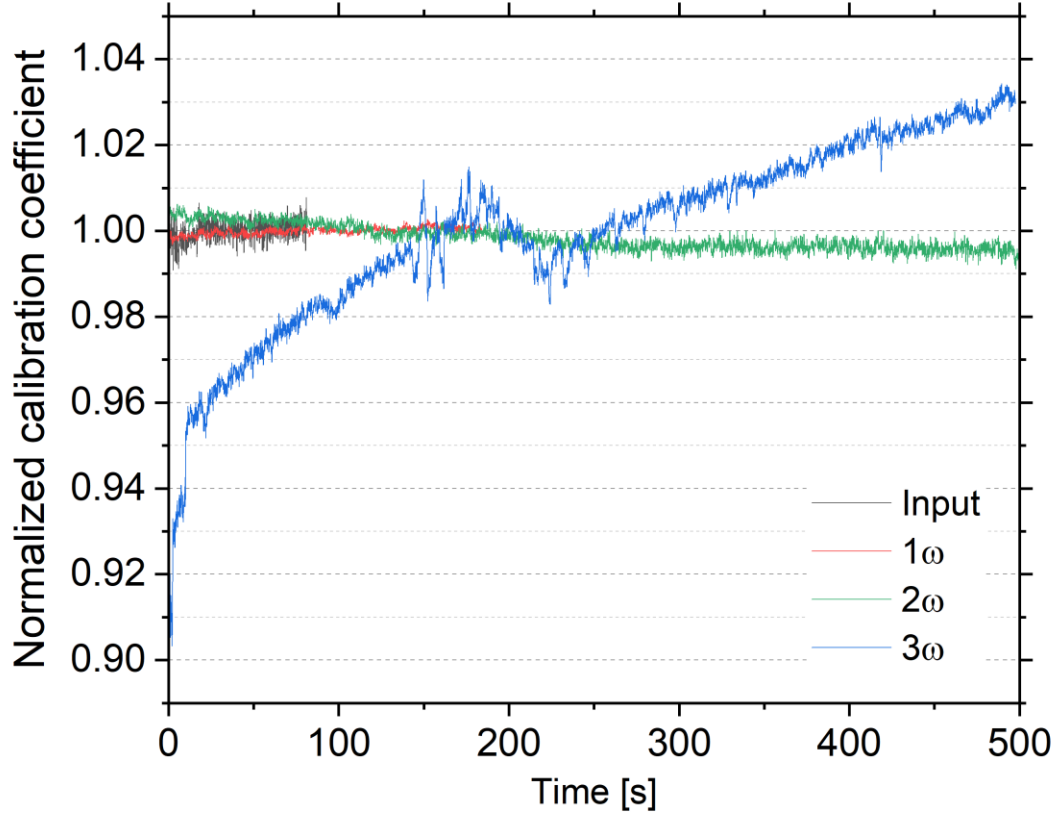


**Figure 2** Temporal evolution of energy meter's calibration coefficients, while calibration coefficient for input energy (1030 nm) and unconverted fundamental  $1\omega$  (1030 nm) stabilized in order of tens of seconds, the second harmonic  $2\omega$  (515 nm) took hundreds of seconds and the third harmonic  $3\omega$  (343 nm) didn't stabilize at all.

By optimizing the input and output polarization of the Bivoj system [9], we increased the polarization uniformity, so that around 96 % of the energy was in polarization suitable for frequency conversion. The  $s$  and  $p$  polarization components of Bivoj beam profile at the input to frequency conversion setup are shown in Figure 3. These results were obtained for the output energy of 92 J, the cooling helium gas flow rate in the main amplifier head was 150 gps and its temperature 120 K.

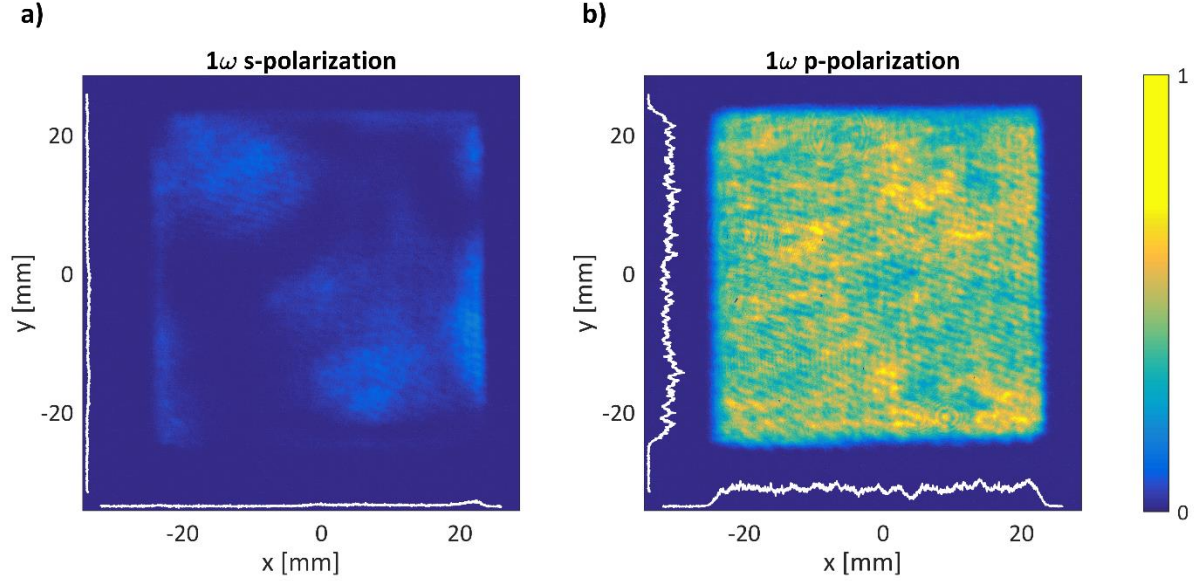


**Figure 3** *S* and *P* component profiles of the laser beam after passage through the demagnifying telescope with optimized polarization at the input and output of the laser system. Images were taken after polarizer transmitting vertical polarization with 4 % of total energy (a) or horizontal polarization with 96 % of total energy (b). Beam profiles at the complementary polarizations were taken under the same conditions and were normalized to sum of both intensities. White lines in the pictures correspond to cross-sections through the center of the beam.

After optimization of polarization uniformity, the LBO crystals were inserted into the position and aligned using low energy beam. The energy was then sequentially increased up to 86.5 J at the input of the first LBO crystal and the phase matching angles of both crystals were optimized to maximize the THG yield. The energy conversion data are shown in Figure 4. The energy of THG at 343 nm reached the value of 55 J and conversion efficiency of 63.5 %. If we counted only the input energy in the p-polarization, that can be converted to second harmonic by the given LBO crystal (i.e., neglect the energy in the unusable polarization), the conversion efficiency would reach 66%.

As shown in the previous work [10] the SHG oven was able to stabilize the temperature of the SHG LBO crystal well, when only the second harmonic was generated. However, after the insertion of THG crystal and optimization of its angle, the SHG conversion efficiency started to deteriorate. We were able to recover most of the SHG and THG performance by adjusting the

phase matching angle of the SHG crystal only. Adjustments of the THG crystal angle had no effect on the resulting THG performance. Based on this observation, we believe that there was parasitic feedback of the 343 nm radiation that caused rapid heating of the SHG crystal and instability of its temperature stabilization control. While the overall temperature increase of the SHG crystal can be compensated by adjusting its phase matching angle, the induced temperature gradients could not be compensated in such way.

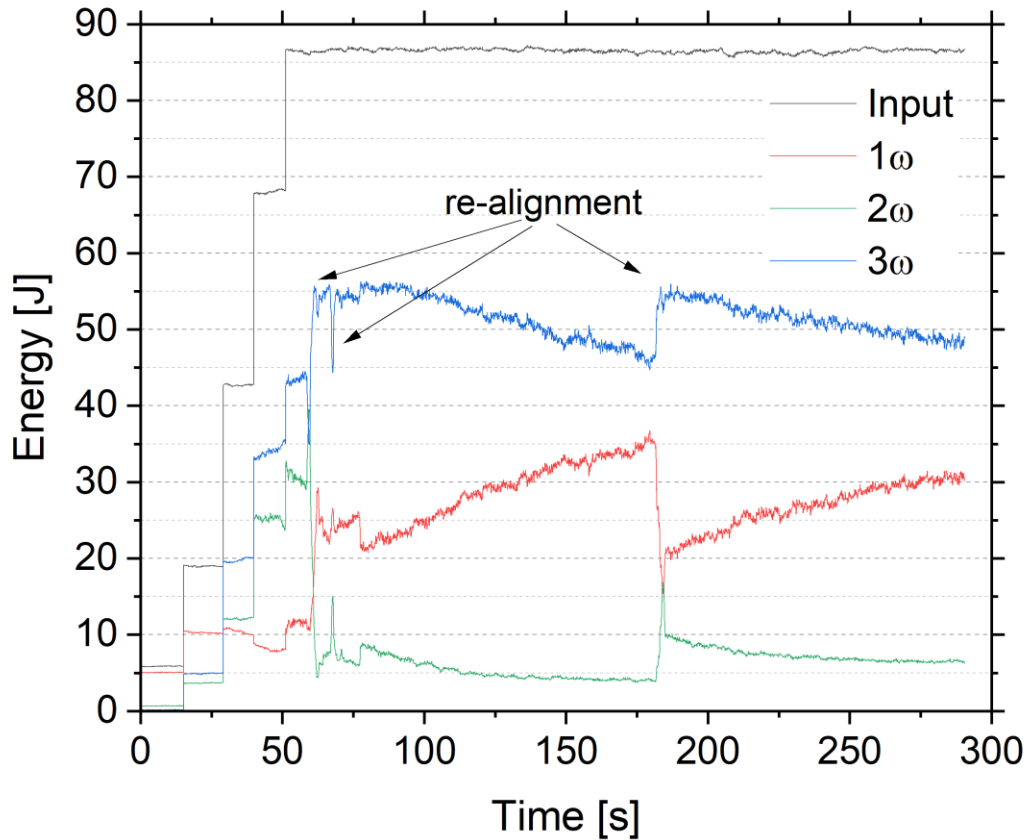
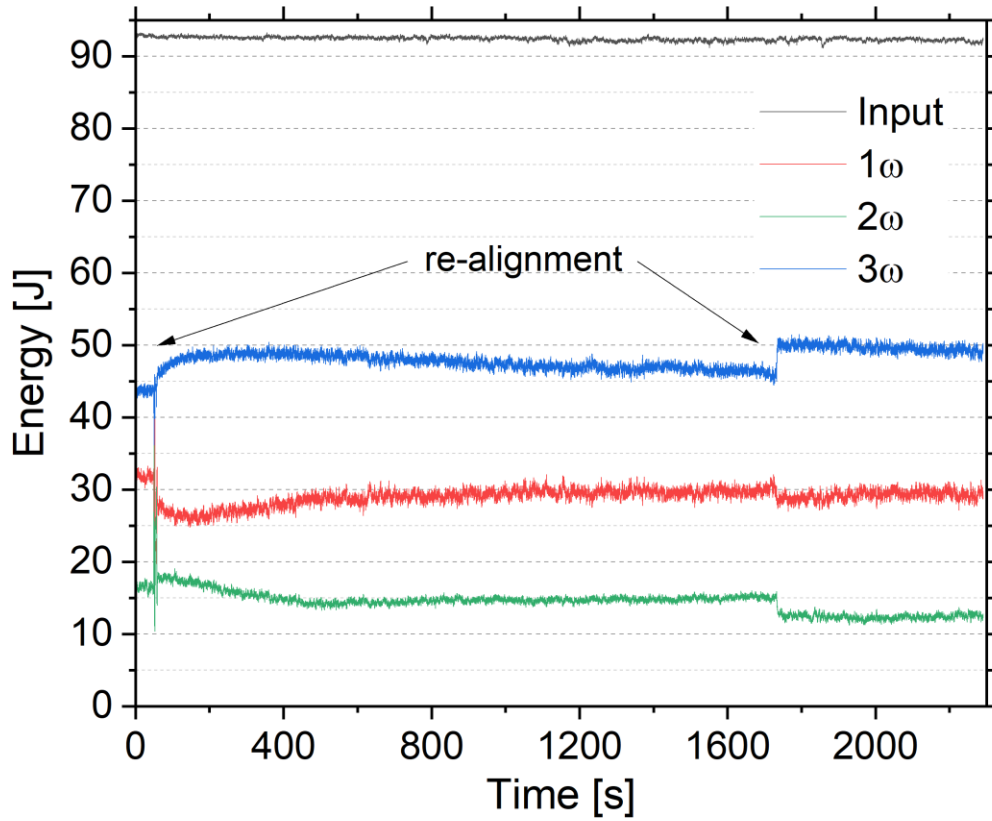


Figure 4 Temporal evolution of the energy of the third harmonic frequency  $3\omega$  together with input energy (1030 nm) and unconverted residual energy on fundamental  $1\omega$  (1030 nm) and second harmonic  $2\omega$  (515 nm) frequencies. Points where crystal phase matching angle was optimized are marked with arrows.

The SHG oven took more than 40 minutes to stabilize the temperature and it required continuous tuning of the phase matching angles to keep the heat sources at constant level. Still, the temperature

stability as well as consequent energy stability was achieved in the end as is shown in Figure 5.

However, the stable output energy at 343 nm dropped to 46-48 J.



**Figure 5** Temporal evolution of the energy of the third harmonic frequency  $3\omega$  (343 nm) together with input energy (1030 nm) and unconverted residual energy on fundamental  $1\omega$  (1030 nm) and second harmonic  $2\omega$  (515 nm) frequencies after SHG oven temperature stabilization.

Final phase matching angles optimization in Figure 4 (around time of 1700 s) increased output energy of 50 J with conversion efficiency of 53.5%. If only the convertible energy is taken into account, the conversion efficiency will increase to 55.5%. This final track is shown in Figure 5 in more details.



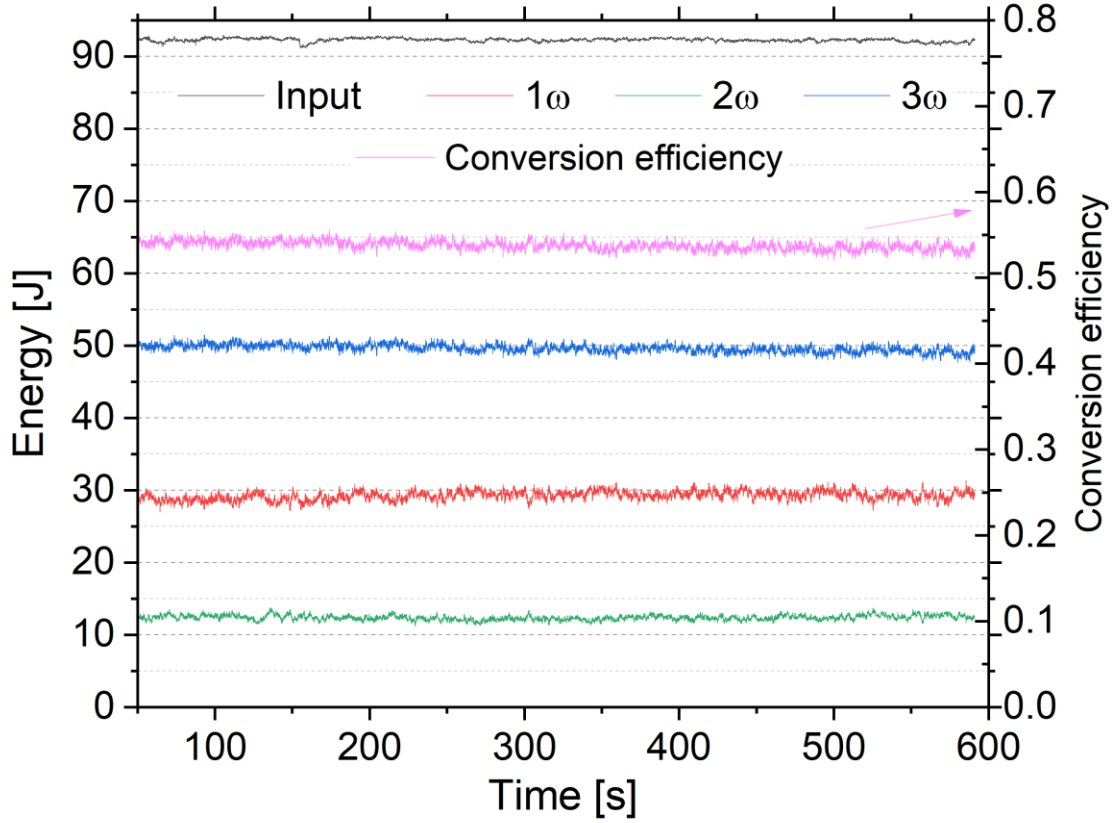


**Figure 6** Temporal evolution of the energy of the third harmonic frequency  $3\omega$  (343 nm) together with input energy (1030 nm) and unconverted residual energy on fundamental  $1\omega$  (1030 nm) and second harmonic  $2\omega$  (515 nm) frequencies after SHG oven temperature stabilization and fine tuning of the SHG LBO phase matching angle. Conversion efficiency is shown in pink and is related to the scale on the right.

The energy stability of the input beam at fundamental frequency was 0.3% RMS and 2.0% P-t-P (peak-to-peak). Energy stability of the third harmonic beam at the beginning of the experiment was 6% RMS and 22% P-t-P (Figure 4, time 75 – 160 s) and was caused by rapid heating of the SHG LBO crystal. After thermalization of the SHG crystal and re-optimization of the SHG phase matching angle, the energy stability improved to 1.1% RMS and 7.5% P-t-P (Figure 5).

The near field beam profile at 343 nm corresponding to energy of 55 J at the beginning of the experiment and 50 J obtained after 90 minutes are shown Figure 7. They show that temperature

gradient was created inside the crystals and conversion efficiency varied over the crystal cross-section.

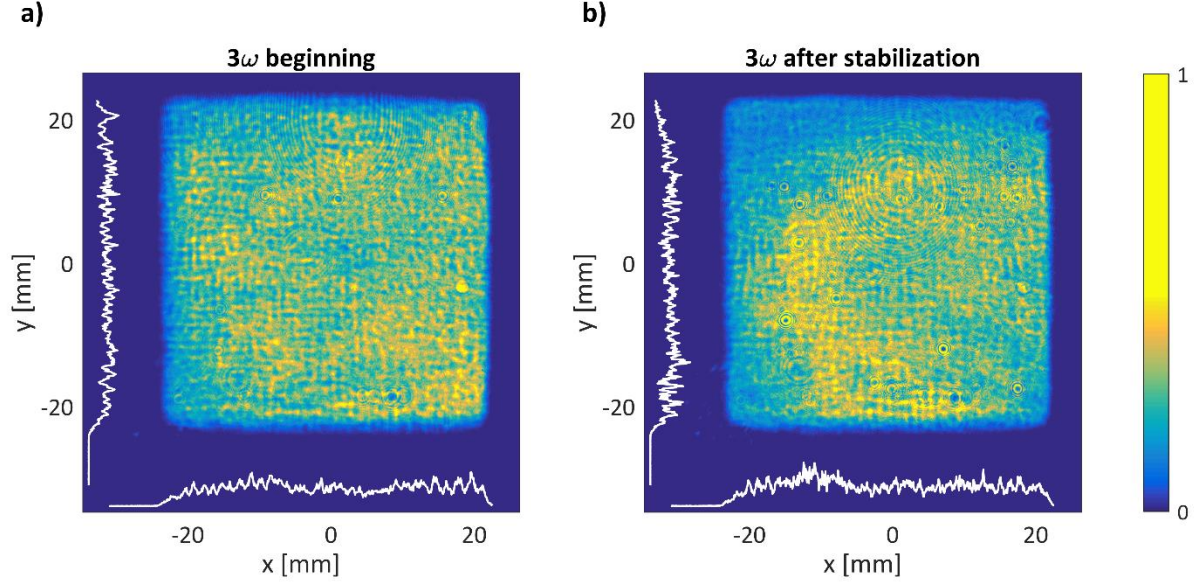


**Figure 7** Beam profile on third harmonic frequency (343 nm) with energy of  $>50$  J at the repetition rate of 10 Hz in the beginning of the experiment (a) and after oven temperature stabilization after 90 minutes (b). The color bar was adjusted to better show the intensity variation in the beam in the presence of hot spots that affected the normalization.

### III. Conclusion

The output of THG of 50 J at 10 Hz at 343 nm was achieved for the first time and it represents 4 times increase to the state-of-the-art. The third harmonic generation process was achieved using two LBO crystals placed in temperature-controlled holders. The output beam profile is square super-gaussian with satisfactory energy uniformity. Long thermalization was required due to strong optical feedback between second and third harmonic generation crystals due to strong reflection from AR coatings. This will be addressed in the continuation of this work. However, after the thermalization, the energy stability of THG output was excellent and reached 1.1% RMS.

### Acknowledgement

European Regional Development Fund and the state budget of the Czech Republic project HiLASE CoE (CZ.02.1.01/0.0/0.0/15\_006/0000674), project LasApp (CZ.02.01.01/00/22\_008/0004573) and Horizon 2020 Framework Programme (H2020) (739573).

## Conflict of Interest

The authors have no conflicts to disclose.

## Data Availability Statement

The data that support the findings of this study are openly available in Zenodo repository at <https://doi.org/10.5281/zenodo.12569726>, reference [12].

## References

1. H. Abu-Shawareb et al., Achievement of Target Gain Larger than Unity in an Inertial Fusion Experiment. *Physical Review Letters*, **132** (2024). <https://doi.org/10.1103/PhysRevLett.132.065102>.
2. W. Han et al., The effect of laser beam size on laser-induced damage performance. *Chinese Physics B*, **21** (2012). <https://doi.org/10.1088/1674-1056/21/7/077901>.
3. J. Y. Natoli, J. Capoulade, H. Piombini, & B. Bertussi, Influence of laser beam size and wavelength in the determination of LIDT and associated laser damage precursor densities in KH 2 PO 4. *Laser-Induced Damage in Optical Materials: 2007* (2007). <https://doi.org/10.1117/12.750142>.
4. Elliott David J., Ultraviolet laser technology and applications. (n.d.) 1 online resource (367 pages) :
5. E. Schubert et al., HV discharge acceleration by sequences of UV laser filaments with visible and near-infrared pulses. *New Journal of Physics*, **19** (2017). <https://doi.org/10.1088/1367-2630/aa9b76>.
6. J. P. Phillips et al., Second and third harmonic conversion of a kilowatt average power, 100-J-level diode pumped Yb:YAG laser in large aperture LBO. *Optics Letters*, **46** (2021). <https://doi.org/10.1364/ol.419861>.
7. J. Rothhardt et al., 100 W average power femtosecond laser at 343 nm. *Optics Letters*, **41** (2016). <https://doi.org/10.1364/ol.41.001885>.
8. U. Andral et al., Second and third harmonic generation from simultaneous high peak- and high average-power thin disk laser. *Applied Physics B: Lasers and Optics*, **128** (2022). <https://doi.org/10.1007/s00340-022-07887-8>.
9. O. Slezák et al., Thermal-stress-induced birefringence management of complex laser systems by means of polarimetry. *Scientific Reports*, **12** (2022). <https://doi.org/10.1038/s41598-022-22698-9>.

10. D. Clarke et al., Improved stability second harmonic conversion of a diode-pumped Yb:YAG laser at the 0.5 kW level. *Optics Letters*, **48** (2023).  
<https://doi.org/10.1364/ol.497181>.
11. M. Divoky et al., Kilowatt-class high-energy frequency conversion to 95 J at 10 Hz at 515 nm. *High Power Laser Science and Engineering*, **11** (2023).  
<https://doi.org/10.1017/hpl.2023.60>.
12. J. Pilar & M. Divoky, Half-kilowatt high energy third harmonic conversion to 50 J @ 10 Hz at 343 nm [dataset]. (2024).  
<https://doi.org/10.5281/zenodo.12569726>.